Improved Value for the Gamow-Teller Strength of the ^{100}Sn Beta Decay

D. Lubos,[1,2] J. Park,[3,4,*] T. Faestermann,[1,5,†] R. Gernhäuser,[1] R. Krücken,[1,3,4] M. Lewitowicz,[6] S. Nishimura,[2] H. Sakurai,[7] D. S. Ahn,[2] H. Baba,[2] B. Blank,[8] A. Blazhev,[9] P. Boutachkov,[10] F. Browne,[2,11] I. Čeliković,[6,12] G. de France,[6] P. Doornenbal,[2] Y. Fang,[13] N. Fukuda,[2] J. Giovinazzo,[8] N. Goel,[10] M. Górska,[10] S. Ilieva,[14] N. Inabe,[2] T. Isobe,[2] A. Jungclaus,[15] D. Kameda,[2] Y. K. Kim,[16,17] I. Kojouharov,[10] T. Kubo,[2] N. Kurz,[10] Y. K. Kwon,[16] G. Lorusso,[2] K. Moschner,[9] D. Murai,[2] I. Nishizuka,[18] Z. Patel,[2,19] M. M. Rajabali,[3,20] S. Rice,[2,19] H. Schaffner,[10] Y. Shimizu,[2] L. Sinclair,[2,21] P.-A. Söderström,[2] K. Steiger,[1] T. Sumikama,[18] H. Suzuki,[2] H. Takeda,[2] Z. Wang,[3] N. Warr,[9] H. Watanabe,[22] J. Wu,[2,23] and Z. Xu[7]

[1]*Physik Department E12, Technische Universität München, D-85748 Garching, Germany*
[2]*RIKEN Nishina Center, 2-1 Hirosawa, Wako, Saitama 351-0198, Japan*
[3]*TRIUMF, Vancouver British Columbia, V6T 2A3, Canada*
[4]*Department of Physics and Astronomy, University of British Columbia, Vancouver, British Columbia V6T 1Z1, Canada*
[5]*Excellence Cluster "Origin and Structure of the Universe", D-85748, Garching, Germany*
[6]*Grand Accélérateur National d'Ions Lourds (GANIL), CEA/DSM-CNRS/IN2P3, Boulevard H. Becquerel, 14076 Caen, France*
[7]*University of Tokyo, 7-3-1 Hongo Bunkyo, Tokyo 113-0033, Japan*
[8]*CEN Bordeaux-Gradignan Le Haut-Vigneau, F-33175 Gradignan Cedex, France*
[9]*Institute of Nuclear Physics, University of Cologne, D-50937 Cologne, Germany*
[10]*GSI Helmholtzzentrum für Schwerionenforschung GmbH, D-64291 Darmstadt, Germany*
[11]*School of Computing, Engineering and Mathematics, University of Brighton, Brighton, BN2 4GJ, United Kingdom*
[12]*"Vinča" Institute of Nuclear Sciences, University of Belgrade, 11000 Belgrade, Serbia*
[13]*Osaka University, 1-1 Machikaneyama, Toyonaka, Osaka 560-0043, Japan*
[14]*Technische Universität Darmstadt, D-64289 Darmstadt, Germany*
[15]*Instituto de Estructura de la Materia, IEM-CSIC, E-28006 Madrid, Spain*
[16]*Rare Isotope Science Project, Institute for Basic Science, Daejeon 305-811, Republic of Korea*
[17]*Department of Nuclear Engineering, Hanyang University, Seoul 133-791, Republic of Korea*
[18]*Department of Physics, Faculty of Science, Tohoku University, Sendai 980-0845, Japan*
[19]*Department of Physics, University of Surrey, Guildford GU2 7XH, United Kingdom*
[20]*Physics Department, Tennessee Technological University, Cookeville, Tennessee 38505, USA*
[21]*University of York, York YO10 5DD, United Kingdom*
[22]*Beihang University, Beijing 100191, China*
[23]*Department of Physics, Peking University, Beijing 100871, China*

(Received 18 February 2019; revised manuscript received 11 April 2019; published 7 June 2019)

A record number of ^{100}Sn nuclei was detected and new isotopic species toward the proton dripline were discovered at the RIKEN Nishina Center. Decay spectroscopy was performed with the high-efficiency detector arrays WAS3ABi and EURICA. Both the half-life and the β-decay end point energy of ^{100}Sn were measured more precisely than the literature values. The value and the uncertainty of the resulting strength for the pure $0^+ \rightarrow 1^+$ Gamow-Teller decay was improved to $\mathcal{B}_{\mathrm{GT}} = 4.4^{+0.9}_{-0.7}$. A discrimination between different model calculations was possible for the first time, and the level scheme of ^{100}In is investigated further.

DOI: 10.1103/PhysRevLett.122.222502

^{100}Sn and its neighboring nuclei comprise a unique testing ground for modern large scale shell model (LSSM) calculations with realistic nuclear interactions. ^{100}Sn is the heaviest doubly magic $N = Z$ nucleus that is particle stable and decays via a pure and very fast Gamow-Teller (GT) β decay. The ^{100}Sn region is located in the nuclear chart close to the end of the astrophysical rapid proton capture process path. Thus, it is of particular interest concerning fundamental challenges in both nuclear physics and astrophysics [1].

According to the extreme single particle model (ESPM) [2], ^{100}Sn decays via a pure GT transition of a proton (π) from the completely filled $\pi 0g_{9/2}$ orbital into a neutron (ν) in the empty spin-orbit partner, the $\nu 0g_{7/2}$ orbital of ^{100}In. The ESPM GT strength is predicted to be $\mathcal{B}_{\mathrm{GT}} = 17.78$ [1]. However, the experimental values obtained up to now are smaller: $9.1^{+3.0}_{-2.6}$ [3] and $5.8^{+5.5}_{-3.2}$ [4,5]. These experiments [3,5,6] revealed the smallest $\log(ft)$ value—even smaller than the values of nuclei which decay by a Superallowed Fermi decay—throughout the nuclear chart. However, the

small number of nuclei available for analysis resulted in large statistical uncertainties, such that a quantitative comparison with various theoretical models was not meaningful. The observed GT strength can be reduced for several reasons. The so-called GT quenching, which is caused by the fact that the high-energy part of the GT resonance (> 60 MeV) [7] is not accessible by β decay, is usually accounted for by renormalization of the weak-coupling constants $G_A/G_V = 1.27$ to unity [1]. Further apparent reduction in the experimental GT strength is due to particle-hole excitations and configuration mixing. Modern LSSM calculations predict higher lying 1^+ states populated with small transition matrix elements leading to fragmentation of the decay strength while preserving one dominant decay channel to the yrast 1^+ state. Considering contributions from up to $5p5h$ excitations, $\mathcal{B}_{\mathrm{GT}}$ values between 5.68 and 8.2 are obtained by Nowacki and Sieja ([3]). Earlier predictions with a smaller configuration space [8] yield similar results. In order to scrutinize theoretical models, a new decay spectroscopy experiment was performed to reduce the statistical uncertainties and improve the knowledge of the ^{100}In level scheme.

The experiment was performed at the Radioactive Ion Beam Factory of the RIKEN Nishina Center by employing a stable ^{124}Xe primary beam with an intensity up to 36 pnA and a kinetic energy of 345 A MeV. The secondary beam was produced by projectile fragmentation in a 4-mm-thick ^{9}Be target. The separation and identification of secondary particles were performed by employing the magnetic separator BigRIPS [9] using the $B\rho$-ΔE-$B\rho$ method [10] and the $B\rho$-ΔE-TOF method at the ZeroDegree spectrometer [9]. The energy loss was measured with a tilted-electrode gas ionization chamber [11] at the final focal plane while the time of flight was determined by using plastic scintillators. The beam tracking as well as fine tuning of the particle identification resolution has been performed by the sophisticated background suppression methods described by Fukuda *et al.* [12].

Approximately 2500 ^{100}Sn nuclei were produced, increasing the available world data by a factor of ∼10. The same holds for the even more exotic nuclei along the $N = Z - 1$ line as well as the newly identified $N = Z - 2$ nuclei ^{96}In, ^{94}Cd, ^{92}Ag, and ^{90}Pd [13,14].

The individually identified secondary beam particles were implanted into a modified WAS3ABi detector array [15]. It consists of three double-sided segmented (60 by 40 strips) and 1-mm-thick Si detectors for implantation, extended by a stack of 10 single-sided segmented (seven strips) and 1-mm-thick Si detectors for the calorimetry of β^+ particles. Both, implantation and decay events, were detected in the same Si detector. The high granularity of the implantation detectors was used to optimize the signal-to-noise ratio by requiring that implantation and decay events had occurred in the same pixel. A veto scintillation detector was set up behind the Si detectors in order to prevent light charged particles (e.g., protons and deuterons), which originate from the fragmentation reaction, from triggering the data acquisition.

The WAS3ABi array was surrounded by 47 HPGe detectors of the high-resolution EURICA detector array [16] (37 of the 84 detectors were not functioning) to detect correlated γ emission. Because of the missing detectors the efficiency was, with 4.6% at 1 MeV, about half of the optimum value. Nevertheless, isomeric spectroscopy, β-delayed γ spectroscopy, and also γ-γ coincidence measurements were possible [14].

The β-decay half-life of ^{100}Sn was determined by two methods: (1) using implantation-decay correlations within a time window $t_c = 10$ s (see Fig. 1, inset top) and (2) employing in addition a coincidence with any of the known gamma transitions in ^{100}In (see Fig. 1, inset bottom). The first data set was analyzed with a binned maximum likelihood (MLH) fit, while the unbinned MLH method was applied for the second data set. Both yield consistent

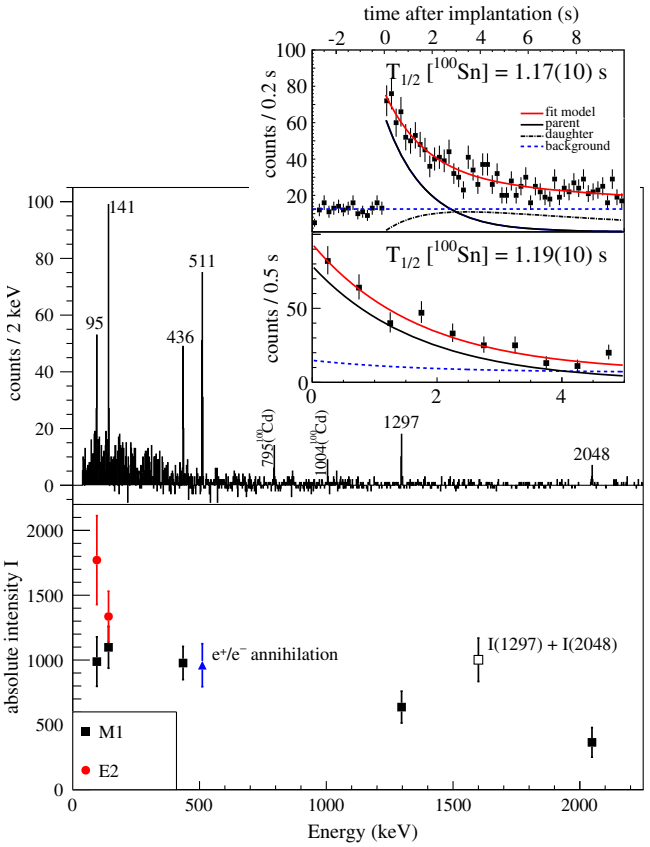

FIG. 1. Top: β-delayed γ spectrum of the ^{100}Sn decay. Uncorrelated background for the same time interval (10 s) was subtracted. Bottom: absolute intensities of γ emission, the 511 keV intensity is divided by two. Inset: decay curves of ^{100}Sn; top: considering all decay correlations, bottom: events gated by the six labeled γ transitions in ^{100}In. The lines show the total fit results which are composed of the ^{100}Sn decay, the background (dashed) and the daughter decay in the case of all decays.

values of 1.17(10) s and 1.19(10) s for the half-life of ^{100}Sn. Because about half of the ungated data are not contained in the gated data, the two results can be combined to 1.18(8) s where the uncertainty of the ungated result is inflated by a factor of $\sqrt{2}$. This compares well with the weighted average of the literature values of 1.10(18) s [3,5,17]. Throughout this Letter, we are using 1σ uncertainties. In method (1), the daughter components are considered according to the Bateman equations [18]. However, the contribution from the β decay of the granddaughter ^{100}Cd is negligible with its half-life of 49.2 s $\gg t_c$. The half-life of the daughter nucleus ^{100}In was determined by a γ-gated event selection. The result of 5.8(2) s is consistent but not as precise as the value 5.62(6) s obtained for the β- and βp-data from this experiment [19]. The random background component was derived from decay events occurring before the implantations and used as a fixed component when implantation-decay correlations were analyzed. In the case of the γ-gated event selection, a second exponential component was considered whose decay constant and amplitude were also derived from events negative in time. Alternatively, this background component was determined with time spectra obtained by setting gates on either side of the γ-ray lines. Both methods yielded identical results. For the γ-gated event selection, we required at least one of the prompt ($t_c^\gamma < 300$ ns) cascading transitions, which are known to depopulate the lowest 1^+ state of ^{100}In, with energies of 2048, 1297, 436, 141, or 95 keV [3].

These known transitions are confirmed by the unprecedented statistics of the β-delayed γ-rays shown in Fig. 1. γ-γ coincidence analysis was possible for the first time (see Fig. 2). It revealed two branches postulated by Hinke *et al.* [3,20]. The transitions with 1297 and 2048 keV both depopulate the lowest 1^+ state of ^{100}In. The branches merge and transitions with 436, 141, and 95 keV are

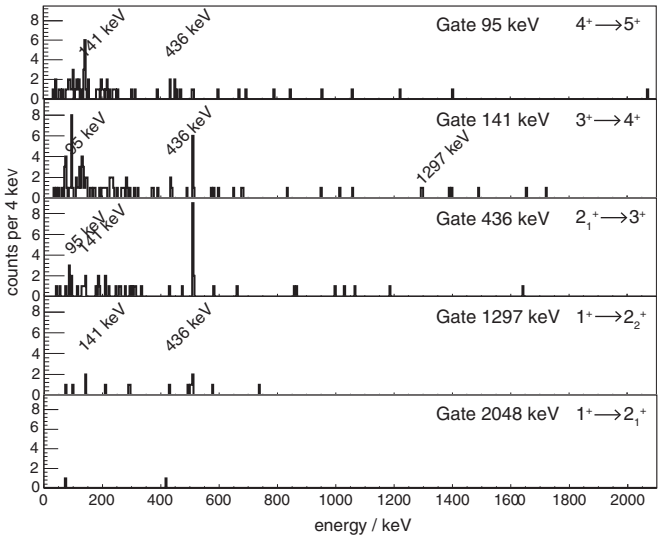

FIG. 2. γ-γ coincidences for transitions in the daughter nucleus ^{100}In.

coincident with both of them. This scenario suggests an unobserved transition to close the gap between the first excited (5^+) state and the expected 6^+ ground state of ^{100}In. Its energy is predicted to be < 50 keV and thus, the transition would be highly converted. However, the energy of its conversion electrons would be lower than the noise level of the Si detectors, such that this transition could not be observed. Only a single coincidence between the lines of 2048 and 95 keV is observed, not sufficient to unambiguously establish the level scheme of ^{100}In.

The conversion probabilities $P_e = [\alpha_{tot}/(1+\alpha_{tot})]$, with the conversion coefficient α_{tot}, were calculated to be 0.371 and 0.164 for the 95 and 141 keV transitions, respectively, assuming $M1$ multipolarity [21]. The observed intensities $N_\gamma(1+\alpha_{tot})/\epsilon(E_\gamma)$, ϵ being the energy dependent γ efficiency (see Fig. 1), have been corrected for this effect. If $E2$ conversion is assumed, the corrected intensities of these transitions would be too large compared with the absolute intensity of e^+e^- annihilation radiation and also with the number of β decays from the half-life analysis. The summed intensity of the 1297 and 2048 keV transitions, depopulating the lowest 1^+ state, is consistent with the intensities of the other transitions and is even 1.04 ± 0.25 times that of the number of positrons, determined from the intensity of the annihilation radiaton. Therefore, there is not much room for feeding of higher lying 1^+ states in the β decay of ^{100}Sn. This is consistent with the prediction of LSSM calculations [3] that the summed $\mathcal{B}_{GT}$ of the β transitions to the next three higher lying 1^+ states is only 30% that of the transition to the lowest 1^+ state, and already a transition energy lower by 700 keV reduces the phase space factor f by a factor of 3. Thus, a γ transition from a 1_2^+ state with 2.75 MeV to the 2_1^+ state and a few % of the intensity of the 2048 keV transition would not have been observable in our experiment.

The second parameter required to determine the Gamow-Teller strength $\mathcal{B}_{GT}$ is the β-decay end point energy Q_β. $\mathcal{B}_{GT}$ scales approximately as Q_β^{-5}. In order to obtain a more accurate Q_β value, a precise energy calibration as well as the understanding of many physical effects is mandatory. In the present experiment, more than 94% of the nuclei of interest have a penetration depth of less than 2 mm in the WAS3ABi array. Thus, β^+ particles emitted in upstream direction with energies > 1 MeV are generally not stopped within the WAS3ABi detectors. In addition, bremsstrahlung and annihilation of the positrons have non-negligible effects on the measured energy distribution, modifying the end point energy by up to 200 keV. This results in a complicated detector response which was studied by means of a GEANT4 simulation [22,23] of the WAS3ABi setup. The average energy loss of positrons (~350 keV/strip), multiple scattering of positrons between Si detector layers, and the aforementioned background processes are the reason why decay events with complete energy deposition and those escaping the detector are indistinguishable. Thus, the

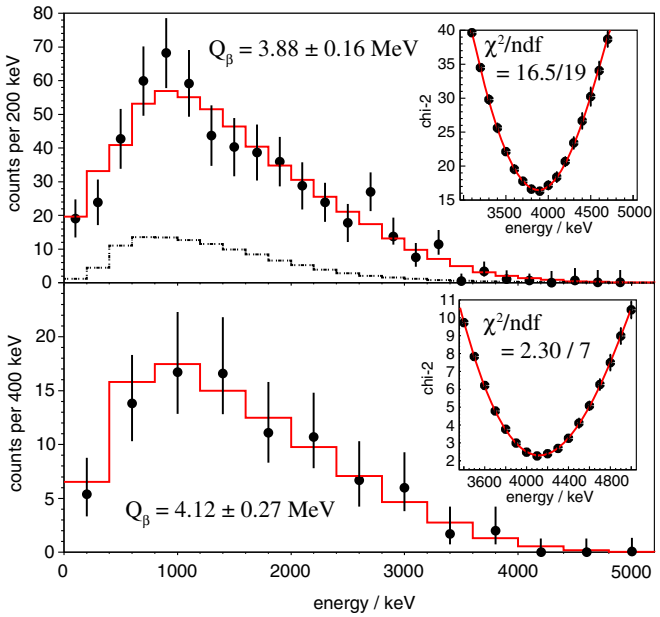

FIG. 3. Top: the energy distribution of positrons after the β decay of ^{100}Sn. Bottom: energy distribution of the γ-gated event selection. The insets show the χ^2 values when comparing the measured spectrum with the simulated spectrum for a certain end point energy. The Q values for the minimal χ^2 are given in the plot and have been used to generate the fully drawn histograms. The dashed histogram represents the contribution of the daughter decay to the spectrum.

energy deposition in all detector channels of WAS3ABi is summed up in each event in order to obtain the experimental β^+ energy distribution (see Fig. 3). Contributions from other processes than β decay such as bremsstrahlung and annihilation radiation are properly considered in the simulation model. Furthermore, the detector energy resolution and internal conversion of the electromagnetic transitions following β^+ decay have also a significant effect on the spectrum shape. They are explored by a Monte Carlo (MC) method where the broadening of the distribution and the occurrence of internal conversion were determined by means of a random distribution. In particular, conversion electrons which trigger the detector readout in electron capture events result in an enhancement of the intensity at energies < 300 keV.

In this Q_β analysis, implantation and decay events were correlated within a time window $t_c \leq 3$ s. As in the half-life analysis, the contribution from the random background was derived from correlations negative in time with $-10\ \text{s} < t_{c,\text{bgd}} < 0$ s. Two Q_β spectra were generated for two data samples: one which considers all decay correlations within the time window and neighboring pixels, and another one under more restrictive conditions which considers only events with implantation and decay in the same pixel which occur coincident with γ-ray emission known to belong to the de-excitation cascade of ^{100}In (see Fig. 3). The confidence intervals of the bin content n_b of the resulting experimental spectra were determined according to Feldman and Cousins [24] if $n_b \leq 20$ or else by $\pm\sqrt{n_b}$. The simulated spectrum was obtained by the same summation method for the energy in the Si detectors because the simulation is considered as an accurate representation of the detector response.

Hence, in order to find which is the best-fitting β-end point energy ϵ_0, simulations were performed for a range of values of ϵ_0. Each simulated data set, normalized to the integral of the experimental spectrum, was compared by means of a χ^2 test with the experimental spectrum. The test was applied to the range where $n_{b,i} > 5$. Then, a polynomial fit of the distribution of χ^2 values was made to determine $Q_\beta \equiv \hat{\epsilon_0}$ where the distribution has its minimum. The 1σ error bounds were determined at $\chi^2 = \chi^2_{\text{min}} + 1$ ([25], Eqs. [29,30]) and the statistical uncertainty of the χ^2 values was obtained by performing a simulation for a given ϵ_0 30 times with a sample size of $N = 10^5$ each. As a consistency check, we applied the same procedure to a β spectrum of ^{98}Cd generated in coincidence with the 1176 keV γ transition which depopulates the lowest 1^+ state in ^{98}Ag. The resulting end point is $Q_\beta = 2.79 \pm 0.08$ MeV. This agrees well with $Q_\beta = 2.717 \pm 0.040$ MeV [26,27].

For ^{100}Sn, the end point energy of the nongated spectrum is obtained as $Q_\beta = 3.88 \pm 0.16$ MeV. This result and the value obtained by the γ-gated sample of $Q_\beta = 4.12 \pm 0.27$ MeV are in agreement and yield an average $Q_\beta = 3.91 \pm 0.15$ MeV, taking into account that about 20% of the total sample are events which are also in the γ-gated sample. Literature values are 3.29 ± 0.20 [3] and $3.8^{+0.7}_{-0.3}$ MeV [5], the former being considerably smaller. The cause for the discrepancy may be due to underestimated systematic uncertainties for the data from the Gesellschaft für Schwerionenforschung (GSI) [3,5] as well as this work which measured the β energy in 2π geometry instead of 4π coverage what required a more elaborate investigation of the detector response from GEANT4 simulations. If we take the weighted average of our and the literature values and inflate the uncertainty by the usual scale factor ([25], p. 15), we arrive at $Q_\beta = 3.71 \pm 0.20$ MeV.

Hence, the ground-state Q_{EC} value, calculated from our data by the sum $Q_\beta + \Delta E_\gamma + \Delta_{e^+e^-}$ with ΔE_γ given by the excitation energy of the populated 1^+ state of ^{100}In (for the unobserved 5^+ to 6^+ transition we assume an energy of 30 ± 30 keV) as well as the annihilation energy $\Delta_{e^+e^-}$, yields 7.69 ± 0.16 MeV. Compared with the Q_{EC} value of 6.9 ± 1.0 MeV from a mass measurement [28], this result is compatible.

In the case of a single pure GT transition, we calculate the Gamow-Teller strength as

$$\mathcal{B}_{\text{GT}} = \frac{2\pi^3\hbar^7 \ln 2}{m_e^5 c^4 G_F^2 V_{ud}^2 (G_A/G_V)^2 f T_{1/2}} = \frac{(3885 \pm 14)\ \text{s}}{f(Z', \epsilon_0) T_{1/2}}$$

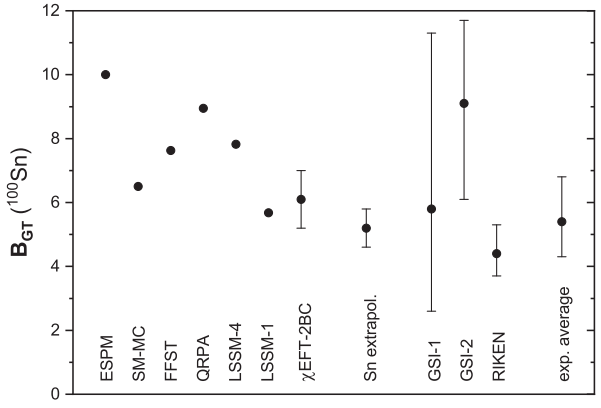

FIG. 4. Comparison of experimental and predicted GT-transition strengths of ^{100}Sn. The theoretical values on the left side are from extreme single particle model [2], shell model—Monte Carlo [32], finite fermi systems theory and quasiparticle random phase approximation [8], large scale shell model with transitions to the four lowest and the lowest 1^+ states [3], the range of recent work explaining GT quenching with calculations using chiral effective field theory combined with two-body currents [31] and the extrapolation from heavier even-even Sn-isotopes [30]. The four points with error bars on the right side are experimental values: the first [5] and second [3] GSI experiments, the present result, and the average of all available data. For the average of Q_β, its error has been inflated by a factor 1.34 to account for the too large χ^2.

where f denotes the phase-space factor with the proton number Z' of the daughter nucleus as its first argument. For the constants we used the 2018 values of the particle data group [25]. The $\log(ft)$ value was calculated to be 2.95 ± 0.08 with the LOGFT calculator [29]. We notice an improved precision but also a larger value compared to the previously most precise value $2.62^{+0.13}_{-0.11}$ by Hinke *et al.* [3]. This results in a lower GT-strength $\mathcal{B}_{\mathrm{GT}} = 4.4^{+0.9}_{-0.7}$ compared to $9.1^{+3.0}_{-2.6}$ [3]. Our new value is consistent with the result $5.8^{+5.5}_{-3.2}$ from the first GSI experiments [4,5]. Furthermore, it is somewhat smaller than the value of 5.7 which is calculated in the LSSM [3] as well as the extrapolation for the summed GT-strength $\mathcal{B}_{\mathrm{GT}} = 5.2(6)$ from heavier even-even Sn isotopes by Batist *et al.* [30] (see Fig. 4). But, comparing the results with the calculations, most of the predicted values overestimate the experimental GT strength and suggest a further reduction. As large model spaces have been used in the most recent LSSM calculations, higher-lying 1^+ states being populated after β decay but being below the detection sensitivity are candidates to carry this fraction of strength. However, recent work [31], explaining GT quenching with calculations using chiral effective field theory combined with two-body currents, obtains for ^{100}Sn a range of $\mathcal{B}_{\mathrm{GT}}$ values between 5.2 and 7.0, quite close to our result and to the LSSM calculations with an empirical quenching factor [3].

In the present experiment, the statistics of implanted ^{100}Sn isotopes was sufficiently large such that a detailed analysis of physical background effects and the detector response could be carried out for the first time. These effects introduce non-negligible systematic uncertainties which have to be carefully taken into account. Eventually, we have determined the GT-transition strength with unprecedented precision by means of decay spectroscopy employing the high resolution detectors WAS3ABi and EURICA. Slight improvements of both, the half-life and the Q_β analysis revealed a dramatic effect on the precision of the GT strength. The value $\mathcal{B}_{\mathrm{GT}} = 4.4^{+0.9}_{-0.7}$ strengthens the arguments of the LSSM calculation to explain the missing strength by the unobserved population of higher-lying states in the daughter nucleus as well as an incomplete model space. A careful gamma-gamma coincidence analysis confirmed the coincidence relations expected on the basis of the proposed level scheme of ^{100}In. However, in spite of an unprecedented number of decay correlations of ^{100}Sn, there was no hint for high-lying 1^+ states in ^{100}In and the suggested transition with $E_\gamma < 50$ keV has not been observed. Concerning the details of the low-energy ^{100}In level scheme, a dedicated experiment with a high γ-ray detection efficiency will be necessary to answer the remaining questions.

This work was carried out at the RIBF operated by RIKEN Nishina Center, RIKEN and CNS, University of Tokyo. It was supported and financed by the DFG cluster of excellence "Origin and Structure of the Universe," the German BMBF under Contracts No. 05P12WOFNF and No. 05P15PKFNA, the Hanns-Seidel-Stiftung, and the RIKEN IPA Programme. We wish to acknowledge the EURICA RIBF09 collaboration as well as the support on the WAS3ABi setup from the Rare Isotope Science Project, funded by the Ministry of Education, Science and Technology and National Research Foundation of Korea-KAKENHI (Grant No. 25247045). Part of the research was also funded by the Natural Sciences and Engineering Research Council of Canada, supported by FJNSP LIA (French-Japanese International Associated Laboratory for Nuclear Structure Problems) and by the Spanish Ministerio de Economía y Competitividad under Contract No. FPA2017-84756-C4-2-P.

*Present address: Department of Physics, Lund University, 22100 Lund, Sweden.
†Corresponding author.
thomas.faestermann@tum.de

[1] T. Faestermann, M. Gorska, and H. Grawe, Prog. Part. Nucl. Phys. **69**, 85 (2013).
[2] A. de Shalit and I. Talmi, *Nuclear Shell Theory* (Academic Press, New York/London, 1963).
[3] C. B. Hinke *et al.*, Nature (London) **486**, 341 (2012), and Supplemental Material.
[4] K. Sümmerer *et al.*, Nucl. Phys. **A616**, 341 (1997).
[5] T. Faestermann *et al.*, Eur. Phys. J. A **15**, 185 (2002).

[6] R. Schneider *et al.*, Phys. Scr. **T56**, 67 (1995).
[7] A. Arima, W. Bentz, T. Suzuki, and T. Suzuki, Phys. Lett. B **499**, 104 (2001).
[8] A. Bobyk, W. A. Kaminski, and I. N. Borzov, Acta Phys. Pol. B **31**, 953 (2000).
[9] T. Kubo *et al.*, Prog. Theor. Exp. Phys. **2012**, 03C003 (2012).
[10] H. Geissel *et al.*, Nucl. Instrum. Methods Phys. Res., Sect. B **70**, 286 (1992).
[11] K. Kimura *et al.*, Nucl. Instrum. Methods Phys. Res., Sect. A **538**, 608 (2005).
[12] N. Fukuda *et al.*, Nucl. Instrum. Methods Phys. Res., Sect. B **317**, 323 (2013).
[13] I. Čeliković *et al.*, Phys. Rev. Lett. **116**, 162501 (2016).
[14] J. Park *et al.*, Phys. Rev. C **97**, 051301(R) (2018).
[15] S. Nishimura *et al.*, RIKEN Accel. Prog. Rep. **46**, 182 (2013).
[16] P.-A. Söderström *et al.*, Nucl. Instrum. Methods Phys. Res., Sect. B **317**, 649 (2013).
[17] D. Bazin *et al.*, Phys. Rev. Lett. **101**, 252501 (2008).
[18] H. Bateman, Proc. Cambridge Philos. Soc. **15**, 423 (1910).
[19] J. Park *et al.*, Phys. Rev. C **99**, 034313 (2019).
[20] See Supplemental Material http://link.aps.org/supplemental/10.1103/PhysRevLett.122.222502 for a copy of the level scheme of ^{100}In from Hinke *et al.*.
[21] T. Kibédi, T. W. Burrows, M. B. Trzhaskovskaya, P. M. Davidson, and C.W. Nestor, Nucl. Instrum. Methods Phys. Res., Sect. A **589**, 202 (2008).
[22] K. Steiger, Effizienzbestimmung des Detektoraufbaus für die Zerfallsspektroskopie von ^{100}Sn, Master's thesis, TUM, 2009.
[23] N. Warr, A. Blazhev, and K. Moschner, EPJ Web Conf. **93**, 07008 (2015).
[24] G. J. Feldman and R. D. Cousins, Phys. Rev. D **57**, 3873 (1998).
[25] M. Tanabashi *et al.* (Particle Data Group), Phys. Rev. D **98**, 030001 (2018).
[26] A. Stolz, Untersuchung des Gamov-Teller-Zerfalls in der Nachbarschaft von ^{100}Sn, Ph.D. thesis, TUM, 2001, GSI-Report DISS. 2001–2009.
[27] A. Stolz *et al.*, GSI-Report-2002-1, 7, 2002.
[28] M. Chartier *et al.*, Phys. Rev. Lett. **77**, 2400 (1996).
[29] M. Emeric and A. Sonzogni, www.nndc.bnl.gov/logft.
[30] L. Batist *et al.*, Eur. Phys. J. A **46**, 45 (2010).
[31] P. Gysbers *et al.*, Nat. Phys. **15**, 428 (2019).
[32] D. Dean, S. Koonin, T. Kuo, K. Langanke, and P. Radha, Phys. Lett. B **367**, 17 (1996).